Int J Adv Manuf Technol (2012) 60:1031–1038
DOI 10.1007/s00170-011-3662-2

ORIGINAL ARTICLE

A new adaptive control chart for monitoring process mean and variability

Jiujun Zhang · Zhonghua Li · Zhaojun Wang

Received: 18 July 2010 / Accepted: 20 September 2011 / Published online: 14 December 2011

Abstract Traditionally, an $\bar{X}$ chart is used to control the process mean, and an R chart is used to control the variance. However, these charts are not sensitive to the small shifts in the processes. The adaptive charts might be considered if the aim is to detect process changes quickly. In this paper, we propose a new adaptive single control chart which integrates the exponentially weighted moving average procedure with the generalized likelihood ratio test statistics for jointly monitoring both the process mean and variability. This new chart is effective in detecting the disturbances that shift the process mean, increase or decrease the process variance, or lead to a combination of both effects.

Keywords Likelihood ratio test · Adjusted average time to signal · Statistical process control

1 Introduction

Statistical process control (SPC) refers to some statistical methods used extensively to monitor and improve the quality of process. In SPC, it is usually necessary to monitor both the process mean and the process variability. Shewhart's $\bar{X}$-R (or $\bar{X}$-S) control charts have been used widely to detect increasing variance and mean shifts in the process, but these charts are not very sensitive to the small shifts in the process and cannot detect the decrease in the variance effectively.

Recently developed adaptive charts have been shown to give substantially faster detection of most process shifts. The chart is adaptive if at least one of the parameters (d, n, h) is allowed to change in real time based on the actual sample point, where d is the sample interval, n is the sample size, and h is the control limit. These adaptive charts include *the variable sampling intervals* (VSI) chart, *the variable sample size* (VSS) chart, *variable sample size and sampling intervals* (VSSI), and *the variable parameter* (VP) chart.

In the operation of adaptive charts, if the current sample point falls in the central region (i.e., the point is close to the target), then it is reasonable to relax the control by waiting more time to take the next sample (i.e., using the long sampling interval d_1), decreasing the size of the next sample (i.e., using small sample size n_1), and /or plotting the next sample point on the chart with wide action limits (i.e., using wide action limit coefficient h_1. On the other hand, if the current sample point falls in the warning region (i.e., the point is far away from the target but still within the action limits), then it is reasonable to tighten the control by waiting less time to take the next sample (i.e., using the short sampling interval d_2), increasing the size of the next sample (i.e., using large sample size n_2), and plotting the next sample point on the chart with narrow action limits (i.e., using narrow action limit coefficient h_2). If the sample point falls outside the action (or control)

Electronic supplementary material The online version of this article (doi:10.1007/s00170-011-3662-2) contains supplementary material, which is available to authorized users.

J. Zhang
Department of Mathematics, Liaoning University, Shenyang 110036, People's Republic of China

Z. Li · Z. Wang (✉)
LPMC and School of Mathematical Sciences, Nankai University, Tianjin 300071, People's Republic of China
e-mail: zjwang@nankai.edu.cn

limits, then the process may be out of control caused by the assignable cause(s).

The vast majority of the research on the adaptive charts has dealt with the analysis of control charts with VSI. Most work on developing VSI control charts focus on monitoring the process mean. The pioneering work of [1] used the $\bar{X}$ chart to introduce the idea of varying the $\bar{X}$ chart sampling interval as a function of what is observed from the process. VSI control charts were also considered by [2–5]. Bai and Lee [6] studied the VSI $\bar{X}$ chart with an improved switching rule. Yang and Su [7] considered the statistical adaptive process control for two dependent process steps. The VSI scheme was extended to cumulative sum (CUSUM) and exponentially weighted moving average (EWMA) charts (see [8–12]). VSS charts were considered, see [13–15]. Subsequently, [16–19] considered VSSI control charts.

Many innovations have been proposed to monitor the process mean and variance simultaneously, see [20–28]. Recently, [29] proposed a new chart for monitoring the process mean and variance based on Shiryaev–Roberts procedure. In the adaptive case, [30] and [31] studied the joint $\bar{X}$ and R charts with VP. Reynolds and Stoumbos [32] investigated three joint charts for monitoring the process mean and variance of a normal quality variable using individual observations and VSI. Costa and Rahim [33] extended their NCS chart to the adaptive case, where all the parameters are variable. Hawkins and Deng [34] proposed two new combination charts which integrate the CUSUM procedure with the generalized likelihood ratio (GLR) and the Fisher statistics, and it is shown that, in addition to the simplicity of a single chart rather than two, the proposed charts have significant performance advantages over the $\bar{X}$ and S chart pair. But the main disadvantage of the Fisher chart, as they pointed out, is that the Fisher method is biased for variance decrease without concomitant shifts in mean.

Recently, [35] proposed a single chart which integrated the EWMA procedure with the GLR test statistics (ELR chart) for jointly monitoring both the process mean and variability. They showed that their chart was sensitive to various types of shifts in the process including the decrease in the variance. As the ELR chart works better than the other charts when the aim is to detect small shifts in the process mean and variance, it seems logical to think that if the ELR chart is combined with the VSI feature, the new chart that is obtained will be more efficient at detecting small shifts in the process. This paper developed a new chart combining the ELR chart with VSI feature, providing that this is highly efficient in terms of adjusted average time to signal (AATS). More detailed studies on other adaptive features, such as VSS and VP, will be left to our future work.

The rest of this paper is organized as follows: In the next section, our proposed adaptive control chart, the VSI chart, is presented. In Section 3, the performance of the proposed chart is evaluated using a bivariate Markov chain model which is compared to another existing procedure. In Section 4, the paper is concluded with a conclusion.

2 Description of the ELR chart with VSI

Let $\mathbf{x}_t = (x_{t1}, \cdots, x_{tn}), t = 1, 2, \cdots$ denote a sequence of samples of size n taken on a quality characteristic X. It is assumed that, for each t, $x_{t1}, \cdots x_{tn}$ are identically and independently distributed observations and the probability distribution of x_{ti} is assumed to be normal with the mean μ_0 and standard deviation σ_0. When a process shift occurs, the process mean and/or standard deviation will change to:

$$\mu_1 = \mu_0 + \delta\sigma_0, \quad \sigma_1 = \gamma\sigma_0,$$

where $\delta \neq 0$ and/or $\gamma \neq 1$. The δ and γ are usually unknown before monitoring. Without loss of generality, we assume $\mu_0 = 0$ and $\sigma_0 = 1$. Let $\bar{x}_t = \sum_{j=1}^{n} x_{tj}/n$ and $S_t^2 = \sum_{j=1}^{n}(x_{tj} - \bar{x}_t)^2/n$ be the tth sample mean and sample variance.

2.1 A brief review of the ELR chart

Firstly, we give a brief review of the ELR chart which has been proposed by [35].

Given a sample $\mathbf{x}_t$, consider the following hypothesis test

$$H_0 : \mu = 0 \text{ and } \sigma = 1 \longleftrightarrow H_1 : \mu \neq 0 \text{ or } \sigma \neq 1.$$

It is straightforward to obtain the generalized likelihood ratio statistic as follows:

$$l_t = n\left(\bar{x}_t^2 + S_t^2 - \ln S_t^2 - 1\right). \tag{1}$$

It can be easily checked that $l_t \xrightarrow{\mathcal{L}} \chi^2(2)$ as $n \to \infty$. For simplicity, the coefficient n and the constant term -1 can be ignored, so we have

$$\mathrm{LR}_t = \bar{x}_t^2 + S_t^2 - \ln\left(S_t^2\right). \tag{2}$$

Define:

$$u_t = \lambda\bar{x}_t + (1-\lambda)u_{t-1}, \tag{3}$$

$$v_t = \lambda S_t^{*2} + (1-\lambda)v_{t-1}, \tag{4}$$

where $S_t^{*2} = \sum_{j=1}^{n}(x_{tj} - u_t)^2/n$, $u_0 = 0$, $v_0 = 1$, and λ is the smoothing parameter satisfying $0 < \lambda < 1$. In

general, a smaller λ leads to a quicker detection of smaller shifts [36].

Finally, substitute u_t and v_t for $\bar{x}_t$ and S_t^2 in Eq. 2 and obtain the charting statistics

$$\mathrm{ELR}_t = u_t^2 + v_t - \ln(v_t), \quad t = 1, 2, \cdots,$$

If $\mathrm{ELR}_t > h$, an alarm is triggered, where $h > 0$ is chosen to achieve a specified in control ARL (IC ARL), which is the expected number of samples before the chart produces a signal. This chart is called the ELR chart, and it still works for the case $n = 1$ due to the definition of v_t.

2.2 The ELR chart with VSI

When the ELR chart proposed by [35] is used for monitoring a process, a sample of size n_0 is randomly chosen every d_0 hours. The adaptive ELR chart is a modification of the ELR chart in which the parameter d is assumed to be a function of the most recent process information. Like other approaches, the scheme discussed here uses only two different samples alternatively depending on the current process status. When the process is likely to be in control, the long sampling interval d_1, i.e., $d_1 > d_0$ will be used. Conversely, when the process seems close to an out of control condition, the short sampling interval d_2, i.e., $d_2 < d_0$ is used. Let h represent the upper control limit for the VSI ELR chart. The interval $(0, h)$ is partitioned into two distinct regions: $(0, g)$ and $[g, h)$, where g represents the warning limit of the VSI ELR chart. The regions defined by $(0, g)$ and $[g, h)$ are called the central and the warning region, respectively. The region above h is the action region of the chart.

The VSI ELR chart policy works as follows:

$$d(t) = \begin{cases} d_1, & \text{if } 0 < \mathrm{ELR}_{t-1} < g, \\ d_2, & \text{if } g \le \mathrm{ELR}_{t-1} < h, \end{cases}$$

where t is the subgroup index, $d(t)$ is the sampling interval, and ELR_{t-1} is the observation of the $(t-1)$th subgroup. If the sample statistic falls in the caution region, an investigation should be initiated to verify whether the process is out of control or whether it is just the occurrence of a false alarm. If it is a true alarm, then a corrective action should be undertaken to find out the assignable cause(s).

2.3 The performance measure and the design of the adaptive ELR chart

The speed with which a control chart detects process mean and/or variance shifts measures its statistical efficiency. When the interval between samples is fixed, the speed can be measured by ARL. If the interval between samples varied from time to time, the performance can be measured by AATS which is the expected value of the time from process shifts to the time when chart signals. When a process is in control, it is desirable that the mean time from the beginning of the process until a signal be long, which guarantees fewer false alarms. When a process is out of control, it is desirable that the mean time from the occurrence of the assignable cause until a signal be short as this guarantees the fast detection of process changes. It is advisable to start the control with the shorter sampling interval, d_2, so the first sample is taken quickly after the process is started in case of start-up problems. During the in-control period, all samples, including the first one, should have probability of p_0 of being small and 1-p_0 of being large, where

$$p_0 = Pr[\mathrm{ELR} < g | \mathrm{ELR} < h].$$

A two-dimensional illustration of the partitioning the central region and the warning region of the VSI ELR chart is shown in Fig. 1.

The design parameters of the VSI ELR chart (d_1, d_2) and (g, h) are chosen, taking into account the constraint in the following equation:

$$d_1 p_0 + d_2(1 - p_0) = d_0.$$

Usually, d_1 should be large and d_2 should be as small as possible. In this paper, we use two dimensional Markov chain to search for the control limit h and the warning limit g for the adaptive charts. From Fig. 1, we can see the illustration of the partitioning the central region and the warning region of our VSI ELR chart.

Table 1 provides the design parameters of several adaptive ELR charts with $\lambda = 0.2$, $n = 5$, and $d_0 = 1$. Here, g_{I1} and g_{I2} denote the warning limits of the VSI ELR charts with the sampling interval (1.9, 0.1) and (1.2, 0.1), respectively.

2.4 Markov chain calibrations the AATS of the VSI ELR chart

To compute the AATS of the VSI ELR chart, the bivariate Markov chain illustrated in [35] can be applied as well but with a modification.

The transition probability matrix, $\mathbf{P} = (p_{ij \to kl})$, is given by

$$\begin{pmatrix} \mathbf{R_0} & (\mathbf{I} - \mathbf{R_0})\mathbf{1} \\ \mathbf{0} & 1 \end{pmatrix},$$

where the submatrix $\mathbf{R_0}$ is the transition probability matrix for IC states; $\mathbf{I}$ is the identity matrix, and $\mathbf{1}$ is a column vector of ones. Let m_0, m_1, m_2, and m_3 be the

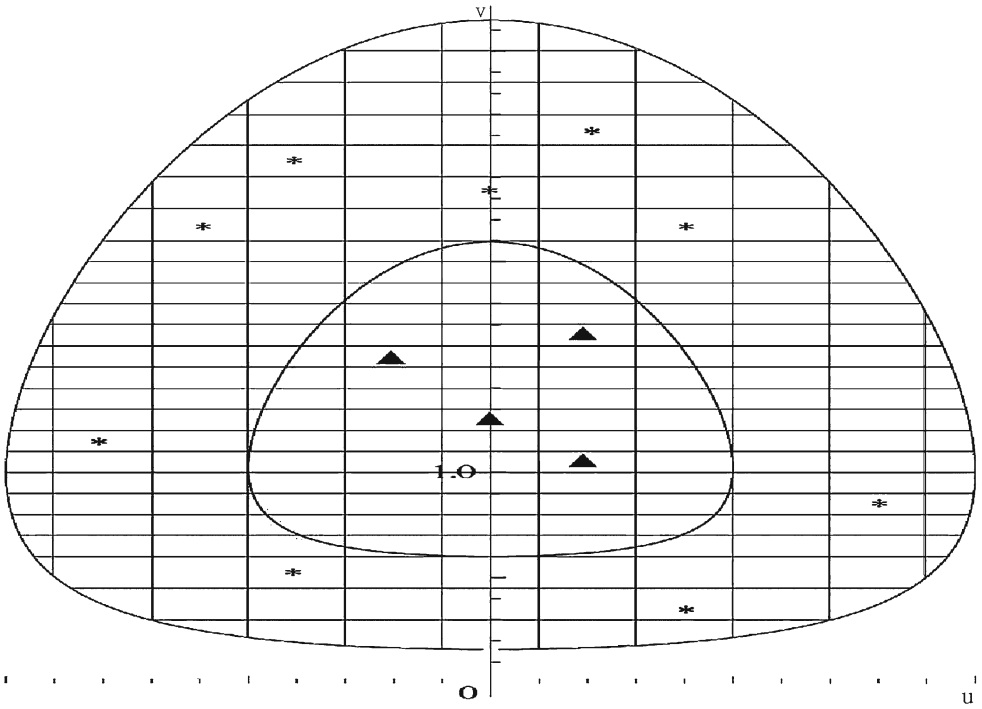

Fig. 1 A two-dimensional illustration of the partitioning of the central region and the warning region of the VSL ELR chart. The notations of *asterisk* and *filled triangle* indicate the points which fall in the warning region and central region, respectively, and indicate the center of this region

given integers. First, we consider the charting statistic of the ELR chart, ELR_t. Note that the function $f(z) = z - \ln z$ is monotonically increase (decrease) when $z > 1$ ($0 < z < 1$) and attains its minimum at $z = 1$. So, from the equation $u^2 + v - \ln(v) = h$, it can be seen that the domain of u is $[-\sqrt{h-1}, \sqrt{h-1}]$ and the domain of v is $[z_1, z_2]$, where z_1, z_2 ($z_1 < z_2$) are the real roots of the equation $z - \ln(z) = h$. Similarly, z_3, z_4 are the real roots of the equation $z - \ln(z) = g$, and $z_1 < z_3 < z_4 < z_2$. Let the number of states along the axis u_t over the interval $[-\sqrt{h-1}, \sqrt{h-1}]$ be $2m_0 + 1$, and then the width of each segment is $w = 2\sqrt{h-1}/(2m_0 + 1)$. Similarly, the axis v_t over the interval $[z_1, z_3)$ is segmented into m_1 states such that the width of each segment is $\Delta_1 = (z_3 - z_1)/m_1$, over the interval $[z_3, z_4)$ is segmented into $m_2 - m_1$ states such that the width of each segment is $\Delta_2 = (z_4 - z_3)/(m_2 - m_1)$, and over the interval $[z_4, z_2]$ is segmented into $m_3 - m_2$ states such that the width of each segment is $\Delta_3 = (z_2 - z_4)(/m_3 - m_2)$. The states along the axis u_t and v_t are, respectively, labeled by $i = -m_0, -m_0 + 1, \cdots, j = 1, 2, \cdots, m_1, m_1 + 1, \cdots, m_2, \cdots, m_3$; thus, the center point of state i along the axis u_t is iw, and the center point of state j along the axis v_t is $z_1 + (j - \frac{1}{2})\Delta_1$ for $j \le m_1$, $z_3 + (j - \frac{1}{2})\Delta_2$ for $m_1 < j \le m_2$, and $z_4 + (j - \frac{1}{2})\Delta_3$ for $m_2 < j \le m_3$.

Table 1 The control limits and warning limits of the VSI ELR charts with $\lambda = 0.2$ and $n = 5$

		IC ARL				
		185	370	400	433	500
FP	h	1.2089	1.2421	1.2460	1.2495	1.2567
VSI	g_{I1}	1.0313	1.0315	1.0315	1.0316	1.0312
	g_{I2}	1.0740	1.0750	1.0750	1.0750	1.0740

Define

$$v(j) = \begin{cases} z_1 + \left(j - \dfrac{1}{2}\right)\Delta_1, & \text{if } 1 \le j \le m_1, \\ z_3 + \left(j - \dfrac{1}{2}\right)\Delta_2, & \text{if } m_1 < j \le m_2, \\ z_4 + \left(j - \dfrac{1}{2}\right)\Delta_3, & \text{if } m_2 < j \le m_3, \end{cases}$$

$$\Delta(j) = \begin{cases} \Delta_1/2, & \text{if } 1 \le j \le m_1, \\ \Delta_2/2, & \text{if } m_1 < j \le m_2, \\ \Delta_3/2, & \text{if } m_2 < j \le m_3, \end{cases}$$

and

$$a(j) = \frac{v(l) - (1-\lambda)v(j) - \Delta(l)}{\lambda},$$

$$b(j) = \frac{v(l) - (1-\lambda)v(j) + \Delta(l)}{\lambda}.$$

Let N_j be such an odd number which is determined by

$$\frac{N_j}{2}\omega < \sqrt{h + \log\left(v(j)^2\right) - v(j)^2},$$

$$\frac{(N_j+1)}{2}\omega > \sqrt{h + \log\left(v(j)^2\right) - v(j)^2},$$

$$j = 1, \cdots, m_3.$$

and N'_j be such an odd number which is determined by

$$\frac{N'_j}{2}\omega < \sqrt{g + \log\left(v(j)^2\right) - v(j)^2},$$
$$\frac{(N'_j+1)}{2}\omega > \sqrt{g + \log\left(v(j)^2\right) - v(j)^2},$$
$$j = m_1 + 1, \cdots, m_2.$$

Denote $\mathbf{R}_{(i,j)\to(k,l)}$ as the transition probability that (u, v) goes from (i, j) to (k, l). Note that

$$S_t^{*2} = \frac{1}{n}\sum_{j=1}^{n}(x_{tj} - u_t)^2 = S_t^2 + (1-\lambda)^2(\bar{x}_t - u_{t-1})^2.$$

Then, when $|i| \le \frac{N_j-1}{2}$, $|k| < \frac{N_l-1}{2}$, the transition probability $\mathbf{R}_{(i,j)\to(k,l)}$ can be evaluated by

$$\begin{aligned}
&\mathbf{R}_{(i,j)\to(k,l)}\\
&= P_r\{(u_t, v_t) = (k, l)|(u_{t-1}, v_{t-1}) = (i, j)\}\\
&= P_r\left\{\left(k-(1-\lambda)i-\frac{1}{2}\right)\frac{w}{\lambda} < \bar{x}_t < \left(k-(1-\lambda)i+\frac{1}{2}\right)\frac{w}{\lambda},\right.\\
&\qquad \left. a(j) < S_t^{*2} < b(j)\right\}\\
&= P_r\left\{\left(k-(1-\lambda)i-\frac{1}{2}\right)\frac{w}{\lambda} < \bar{x}_t < \left(k-(1-\lambda)i+\frac{1}{2}\right)\frac{w}{\lambda},\right.\\
&\qquad a(j) - (1-\lambda)^2(\bar{x}_t - iw)^2 < S_t^2\\
&\qquad \left. < b(j) - (1-\lambda)^2(\bar{x}_t - iw)^2\right\}. \qquad (5)
\end{aligned}$$

Similarly, when $|i| \le \frac{N_j-1}{2}$, $k = -\frac{N_l-1}{2}$, we have

$$\begin{aligned}
&\mathbf{R}_{(i,j)\to(k,l)}\\
&= P_r\{(u_t, v_t) = (k, l)|\,(u_{t-1}, v_{t-1}) = (i, j)\}\\
&= P_r\left\{\frac{-\sqrt{h + \log\left(v^2(j)\right) - v^2(j)} - (1-\lambda)w}{\lambda}\right.\\
&\qquad < \bar{x}_t < \left(1-(1-\lambda)i-\frac{N_l}{2}\right)\frac{w}{\lambda},\\
&\qquad a(j) - (1-\lambda)^2(\bar{x}_t - iw)^2 < S_t^2\\
&\qquad \left. < b(j) - (1-\lambda)^2(\bar{x}_t - iw)^2\right\}. \qquad (6)
\end{aligned}$$

When $|i| \le \frac{N_j-1}{2}$, $k = \frac{N_l-1}{2}$, we have

$$\begin{aligned}
&\mathbf{R}_{(i,j)\to(k,l)}\\
&= P_r\{(u_t, v_t) = (k, l)|(u_{t-1}, v_{t-1}) = (i, j)\}\\
&= P_r\left\{\left(\frac{N_l}{2}-(1-\lambda)i-1\right)\frac{w}{\lambda} < \bar{x}_t\right.\\
&\qquad < \frac{\sqrt{h + \log\left(v^2(j)\right) - v^2(j)} - (1-\lambda)w}{\lambda},\\
&\qquad a(j) - (1-\lambda)^2(\bar{x}_t - iw)^2 < S_t^2\\
&\qquad \left. < b(j) - (1-\lambda)^2(\bar{x}_t - iw)^2\right\}. \qquad (7)
\end{aligned}$$

In other cases, $\mathbf{R}_{(i,j)\to(k,l)} = 0$.

The evaluation of above probabilities involves the following double integral:

$$\int_a^b\int_c^d \phi(x)\chi(y)\mathrm{d}y\mathrm{d}x.$$

Here, in Eq. 5,

$$a = \left[\sqrt{n}\left(k-(1-\lambda)i-\frac{1}{2}\right)\right]\frac{w}{\lambda},$$
$$b = \left[\sqrt{n}\left(k-(1-\lambda)i+\frac{1}{2}\right)\right]\frac{w}{\lambda},$$
$$c = n\left[\frac{1-(1-\lambda)v(j)}{\lambda} - (1-\lambda)\left(\frac{x}{\sqrt{n}} - iw\right)^2\right],$$
$$d = n\left[\frac{1-(1-\lambda)v(j)+\frac{\Delta_2}{2}}{\lambda} - (1-\lambda)\left(\frac{x}{\sqrt{n}} - iw\right)^2\right],$$

In Eqs. 6 and 7, c, d are the same as in Eq. 5, while in Eq. 6,

$$a = \sqrt{n}\left(\frac{-\sqrt{h + \log\left(v^2(j)\right) - v^2(j)} - (1-\lambda)w}{\lambda}\right),$$
$$b = \sqrt{n}\left(1-(1-\lambda)i-\frac{N_l}{2}\right)\frac{w}{\lambda},$$

and in Eq. 7, we have

$$a = \sqrt{n}\left(\frac{N_l}{2}-(1-\lambda)i-1\right)\frac{w}{\lambda},$$
$$b = \sqrt{n}\left(\frac{\sqrt{h + \log\left(v^2(j)\right) - v^2(j)} - (1-\lambda)w}{\lambda}\right),$$

where $\phi(\cdot)$ and $\chi(\cdot)$ are the probability density functions of the standard normal and chi-square with $n-1$ degrees of freedom distributions, respectively. Let $\mathbf{d}$ be a $N \times 1$ vector, the ith element of this vector

corresponds to the interval being taken after the control statistics fall inside the state, i. The approach to determine $\mathbf{d}$ is as follows: First, the number of states N equals $\sum_{j=1}^{m_3} N_j$; also the state (i, j) can be labeled by

$$\sum_{k=0}^{j-1} N_k + \frac{(N_j - 1)}{2} + i + 1,$$

where $i = -\frac{(N_j-1)}{2}, \cdots, 0, \cdots, \frac{(N_j-1)}{2}$, $j = 1, \cdots, m_3$ and $N_0 = 0$. When $m_1 < j \le m_2$ and $|i| \le \frac{N'_j-1}{2}$, or when $|i| = \frac{N'_j+1}{2}$ and $(iw)^2 + v^2(j) - \log(v^2(j)) < g$, which means that the current sample falls in the central region, the corresponding element of $\mathbf{d}$ is d_1. The other elements of $\mathbf{d}$ is d_2, which means that the current sample falls in the warning region. Denote π to be the normalized eigenvector subject to $\pi' R_0 = \pi'$.

Suppose that α is the vector of starting probabilities, then it can be expressed in matrix notation, $\alpha' = \frac{\pi'\mathbf{D}}{\pi'\mathbf{d}}$, where $\mathbf{D}$ is a diagonal matrix with $\mathbf{d}$ on the diagonal. Then the AATS can be expressed as

$$\text{AATS} = \alpha' \left[(\mathbf{I} - \mathbf{R})^{-1} - \frac{1}{2}\mathbf{I} \right] \mathbf{d},$$

where $\mathbf{R}$ is a $N \times N$ dimension matrix when the process is out of control.

3 Performance comparisons

First, we give a brief review of the NCS chart. When the NCS chart proposed by [23] is used for monitoring a process, a sample of size n_0 is randomly chosen every d_0 hours. Then, the values of Y from each sample plotted on the NCS chart with an upper control limit given by $\theta\sigma_0^2$,

$$Y = \sum_{j=1}^{n} (X_j - \mu_0 + \xi\sigma_0)^2.$$

The design parameter ξ is a function of the sample mean. If $\bar{X} > \mu_0$, $\xi = \tau$; otherwise, $\xi = -\tau$, where τ is a positive constant. In general, larger values of τ are better for detecting shifts in μ with $\sigma = \sigma_0$ and worse for detecting increases in σ with $\mu = \mu_0$. A signal is given if $Y > \theta\sigma_0^2$. In this paper, we assumed that $\mu_0 = 0$ and $\sigma_0 = 1$.

AATS results are given for one symmetric and one asymmetric sampling intervals in Table 2. We can see that the more widely spaced intervals yield smaller values of the AATS. The results presented here are fairly consistent with previous research on univariate VSI control charts. In general, the interval d_2 should be as small as possible for better statistical performance [8]; therefor, it usually depends on how soon it is feasible to sample again after the current sample was obtained. On the other hand, the sampling interval d_1

Table 2 AATS for the VSI ELR charts for different intervals when $n = 5$, $\lambda = 0.2$, and IC ARL = 433

		γ							
δ		0.25	0.50	0.75	1.00	1.25	1.50	1.75	2.00
0.00	(1.9, 0.1)	1.5	2.0	5.7	433	12.5	2.8	1.5	1.1
	(1.2, 0.1)	1.9	2.6	8.5	433	15.3	3.6	1.8	1.3
0.25	(1.9, 0.1)	1.5	1.9	4.0	22.2	7.0	2.5	1.5	1.1
	(1.2, 0.1)	1.9	2.5	5.6	28.1	8.8	3.2	1.7	1.2
0.50	(1.9, 0.1)	1.4	1.7	2.5	3.8	3.1	2.0	1.3	1.0
	(1.2, 0.1)	1.8	2.3	3.3	5.0	4.0	2.4	1.6	1.0
0.75	(1.9, 0.1)	1.4	1.5	1.7	2.0	1.8	1.5	1.1	0.9
	(1.2, 0.1)	1.7	1.9	2.2	2.5	2.3	1.7	1.3	1.0
1.00	(1.9, 0.1)	1.2	1.2	1.3	1.3	1.2	1.1	1.0	0.8
	(1.2, 0.1)	1.5	1.5	1.6	1.7	1.5	1.3	1.1	0.9
1.50	(1.9, 0.1)	0.7	0.7	0.7	0.7	0.7	0.7	0.7	0.6
	(1.2, 0.1)	1.0	1.0	0.9	0.9	0.9	0.8	0.8	0.7
2.00	(1.9, 0.1)	0.5	0.5	0.5	0.5	0.5	0.5	0.5	0.5
	(1.2, 0.1)	0.6	0.6	0.6	0.6	0.6	0.6	0.6	0.6

Table 3 ARL, AATS, and PR_i for the FP and adaptive NCS charts and the FP and adaptive ELR charts

$n = 5$		FP			VSI		
δ	γ	NCS	ELR	$PR_1(\%)$	NCS	ELR	$PR_2(\%)$
0.0	1.0	433	433	0.0	433	433	0.0
	1.2	52.6	32.7	37.8	42.8	25.8	39.7
	1.4	14.7	8.6	41.5	9.6	5.4	43.7
	1.6	6.5	4.4	32.3	3.5	2.6	25.7
	1.8	3.8	2.8	26.3	1.8	1.7	5.5
0.2	1.0	225	64.9	71.2	217	48.1	81.5
	1.2	39.0	20.9	46.3	30.7	14.7	52.1
	1.4	12.7	7.7	39.3	8.1	4.7	42.0
	1.6	6.0	4.2	30.0	3.2	2.5	21.9
	1.8	3.6	2.7	25.0	1.8	1.6	11.1
0.4	1.0	76.4	15.5	79.7	65.4	8.3	87.3
	1.2	21.0	10.5	50.0	15.1	6.2	58.9
	1.4	9.0	5.8	35.5	5.4	3.4	37.0
	1.6	5.0	3.6	28.0	2.6	2.2	15.4
	1.8	3.3	2.5	24.2	1.6	1.5	6.2
0.6	1.0	28.2	7.6	73.0	19.9	3.6	81.9
	1.2	11.1	6.1	45.0	6.9	3.3	52.1
	1.4	6.0	4.3	28.3	3.3	2.5	24.2
	1.6	3.9	3.1	20.5	2.0	1.8	10.0
	1.8	2.8	2.2	21.4	1.3	1.3	0.0
0.8	1.0	12.0	4.7	60.8	6.6	2.2	66.7
	1.2	6.3	4.1	34.9	3.3	2.1	36.4
	1.4	4.1	3.2	22.0	2.1	1.8	14.3
	1.6	3.0	2.5	16.7	1.5	1.5	0.0
	1.8	2.4	2.0	16.7	1.1	1.2	−9.0
1.0	1.0	5.9	3.3	44.1	2.6	1.6	38.5
	1.2	3.9	3.0	23.1	1.8	1.6	11.1
	1.4	2.9	2.5	13.8	1.4	1.4	0.0
	1.6	2.4	2.0	16.7	1.1	1.2	−10.0
	1.8	2.0	1.7	15.0	1.0	1.0	0.0

should be chosen to be long so that the resulting control chart would have an acceptable average sampling rate. Similar conclusions can be obtained for other types of changes as well.

Table 3 provides the AATS values for the NCS and the ELR charts with fixed and variable parameters, $d_1 = 1.2$, $d_2 = 0.1$, and it also provides the percentage reduction in detection time (denoted by PR_1 and PR_2) of the ELR and VSI ELR charts relative to the NCS and VSI NCS charts, respectively, where the expressions for PR_i, $i = 1, 2$, are given by

$$PR_i = \left[\frac{AATS_{C_i/NCS} - AATS_{C_i/ELR}}{AATS_{C_i/NCS}}\right], i = 1, 2$$

and where $C_1 = FP$ and $C_2 = VSI$.

From Table 3 we can see that the ELR chart almost always significantly performs better than the NCS chart with or without the VSI feature. Obviously, adding the VSI feature can provide quite substantial reductions in the time required to detect small and moderate shifts. For example, when $\delta = 0.4$ and $\gamma = 1.2$, the AATS values for the NCS and the ELR charts are, respectively, 21.0 and 10.5; for the same shift, the AATS values for the VSI schemes for both charts are 15.1 and 6.2, respectively.

4 Conclusions and considerations

In this paper, we have proposed and studied a single chart for the surveillance of both the process mean and/or variance with VSI procedure. The new chart can be easily designed and constructed, and it is very effective for diverse cases, including the detection of the decrease in the variance which is also very important in many practical applications. The VSI ELR charts and the FP ELR chart were compared to the VSI and FP NCS charts. The conclusion is that the adaptive ELR chart can always detect process disturbance much faster than the NCS charts in detecting small to moderate shifts.

In using VSI ELR chart, we recommend using the shorter sampling interval in the first few samples since the effect of using small sampling intervals is useful at start-up and has more advantages than the fast initial response feature [37] which can result in short IC ARL (and AATS) values.

Acknowledgements The authors are grateful to the editor and the anonymous referees for their valuable comments that have vastly improved this paper. This research was supported by the NNSF of China Grant 11071128, 11131002 and 11101198 and the Fundamental Research Funds for the Central University 65012231.

References

1. Reynolds MR Jr, Amin RW, Arnold JC, Nachlas JA (1998) $\bar{X}$ charts with variable sampling intervals. Technometrics 30:181–192
2. Runger GC, Pignatiello JJ Jr (1991) Adaptive sampling for process control. J Qual Technol 23:135–155
3. Amin RW, Miller RW (1993) A robustness study of $\bar{X}$ charts with variable sampling intervals. J Qual Technol 25:36–44
4. Runger GC, Montgomery DC (1993) Adaptive sampling enhancement for Shewhart control charts. IIE Trans 25:41–51
5. Reynolds MR Jr, Arnold JC, Baik JW (1996) Variable sampling interval $\bar{X}$ charts in the presence of correlation. J Qual Technol 28:1–28
6. Bai DS, Lee KT (2002) Variable sampling interval $\bar{X}$ charts with an improved switching rule. Int J Prod Econ 92:61–74
7. Yang S, Su H (2007) Adaptive sampling interval cause-selecting control charts. Int J Adv Manuf Technol 31:1169–1180
8. Reynolds MR Jr, Amin RW, Amold JC (1990) CUSUM charts with variable sampling intervals. Technometrics 32:371–384
9. Saccucci MS, Amin RW, Lucas JM (1992) Exponentially weighted moving average control charts with variable sampling intervals. Commun Stat Simul Comput 21:627–657
10. Reynolds MR Jr (1996) Shewhart and EWMA variable sampling interval control charts with sampling at fixed times. J Qual Technol 21:199–212
11. Epprecht EK, Simões BFT, Mendes FCT (2010) A variable sampling interval EWMA chart for attributes. Int J Adv Manuf Technol 49:281–292
12. Ou Y, Wu Z, Yu F, Shamsuzzaman M (2010) An SPRT control chart with variable sampling intervals. Int J Adv Manuf Technol 56:1149–1158
13. Prabhu SS, Runger GC, Keats JB (1993) An adaptive sample size $\bar{X}$ charts. Int J Prod Res 31:2895–2909
14. Costa AFB (1994) $\bar{X}$ charts with variable sample size. J Qual Technol 26:155–163
15. Zhang S, Wu Z (2007) A CUSUM scheme with variable sample sizes for monitoring process shifts. Int J Adv Manuf Technol 33:977–987
16. Prabhu SS, Montgomery DC, Runger GC (1994) A combined adaptive sample size and sampling interval $\bar{X}$ control scheme. J Qual Technol 26:164–176
17. Costa AFB (1997) $\bar{X}$ charts with variable sample sizes and sampling intervals. J Qual Technol 29:197–204
18. Celano G, Costa A, Fichera S (2006) Statistical design of variable sample size and sampling interval $\bar{X}$ control charts with run rules. Int J Adv Manuf Technol 28:966–977
19. Mahadik SB, Shirke DT (2011) A special variable sample size and sampling interval Hotelling's T^2 chart. Int J Adv Manuf Technol 53:379–384
20. Gan FF (1995) Joint monitoring of process mean and variance using exponentially weighted moving average control charts. Technometrics 37:446–453
21. Albin SL, Kang L, Sheha G (1997) An X and EWMA chart for individual observations. J Qual Technol 29:41–48
22. Chen G, Cheng SW, Xie H (2001) Monitoring process mean and variability with one EWMA chart. J Qual Technol 33:223–233
23. Costa AFB, Rahim MA (2004) Monitoring process mean and variability with one non-central chi-square chart. J Appl Stat 31:1171–1183
24. Costa AFB (2005) The non-central chi-square chart with double sampling. Braz J Oper Prod Manag 2(3):21–37

25. Costa AFB (2006) The non-central chi-square chart with two stage samplings. European J Oper Res 17:64–73
26. Costa AFB, Rahim MA (2006) A single EWMA chart for monitoring process mean and process variance. Qual Technol Quant Manag 3(3):295–305
27. Costa AFB, Rahim MA (2006) A synthetic control chart for monitoring the process mean and variance. J Qual Maint Eng 12(1):81–88
28. Costa AFB, De Magalhaes MS (2007) An adaptive chart for monitoring the process mean and variance. Qual Reliab Eng Int 23:821–831
29. Zhang J, Zou C, Wang Z (2011) A new chart for detecting the process mean and variability. Commun Stat Simul Comput 40:728–743
30. Costa AFB (1998) Joint $\bar{X}$ and R charts with variable parameters. IIE Trans 30:505–514
31. Costa AFB (1999) Joint $\bar{X}$ and R charts with variable sample size and sampling intervals. J Qual Technol 31:387–397
32. Reynolds MR, Stoumbos ZG (2001) Monitoring process mean and variance using individual observations and variable sampling intervals. J Qual Technol 33:181–205
33. Costa AFB, Rahim MA (2007) An adaptive chart for monitoring the process mean and variance. Qual Reliab Eng Int 23:821–831
34. Hawkins DM, Deng Q (2009) Combined charts for mean and variance information. J Qual Technol 41:415–425
35. Zhang J, Zou C, Wang Z (2010) A control chart based on likelihood ratio test for monitoring process mean and variability. Qual Reliab Eng Int 26:63–73
36. Lucas JM, Saccucci MS (1990) Exponentially weighted moving average control schemes: properties and enhancement. Technometrics 34:46–53
37. Lucas JM, Crosier RB (1982) Fast initial response for CUSUM quality control schemes, give your CUSUM a head start. Technometrics 24:199–205